

# Polymorphism of Gadolinium Diethylenetriaminepentaacetic Acid Bis(methylamide) (GdDTPA-BMA) and Dysprosium Diethylenetriaminepentaacetic Acid Bis(methylamide) (DyDTPA-BMA)

Audun Aukrust,<sup>a,\*</sup> Åse Raknes,<sup>a</sup> Carl E. Sjøgren<sup>a</sup> and Leiv K. Sydnes<sup>b</sup>

<sup>a</sup>Nycomed Imaging AS, PO Box 4220 Torshov, N-0401 Oslo, Norway and <sup>b</sup>Department of Chemistry, University of Bergen, Allégt. 41, N-5007 Bergen, Norway

Aukrust, A., Raknes, Å., Sjøgren, C. E. and Sydnes, L. K., 1997. Polymorphism of Gadolinium Diethylenetriaminepentaacetic Acid Bis(methylamide) (GdDTPA-BMA) and Dysprosium Diethylenetriaminepentaacetic Acid Bis(methylamide) (DyDTPA-BMA). – Acta Chem. Scand. 51: 918–926. © Acta Chemica Scandinavica 1997.

The polymorphism of the title compounds, two paramagnetic metal complexes used for magnetic resonance imaging, has been investigated. Both GdDTPA-BMA (IUPAC name: Aqua[*N,N*-bis[2-[(carboxymethyl)](methylcarbamoyl)methyl]amino]ethyl]glycinato(3-)]gadolinium, hydrate) and DyDTPA-BMA (IUPAC name: Aqua[*N,N*-bis[2-[(carboxymethyl)](methylcarbamoyl)methyl]amino]ethyl]glycinato(3-)]dysprosium, hydrate) can exist in five different polymorphs and as amorphous material. The polymorphs have been characterized by IR, Raman, powder X-ray and DSC/TGA techniques and by measurement of water content and water solubility. The interconversion between the different polymorphs has been studied by exposing samples of the different types to different humidity and temperature conditions. All metastable forms are converted to the thermodynamically most stable form under appropriate conditions.

Dedicated to Professor Lars Skattebøl on the occasion of his 70th birthday.

Polymorphism is commonly understood as the ability of a compound or an element to crystallize in more than one distinct crystal structure. Each crystalline form of such a compound is called a polymorph.<sup>1</sup> Polymorphs of a given substance can be as dissimilar in structure and properties as the crystals of two different compounds.<sup>2–4</sup> This is reflected by the fact that the dissolution rate, solubility, vapour pressure, melting point, density, hardness, crystal shape and optical and electrical properties may vary with the polymorphic form.<sup>5</sup> However, these differences disappear in the liquid or vapour state. The thermodynamically most stable polymorph of a compound, usually named type I,<sup>1</sup> generally has the highest melting point and the lowest solubility. The other polymorphs are metastable and capable of being converted into the most stable form. Pseudopolymorphs occur by loss or gain of solvent without the formation of a new polymorph. Except for solvent content pseudopolymorphs have identical properties. In some cases the phenomenon of polymorphism may be difficult to reproduce.<sup>6</sup>

\* To whom correspondence should be addressed.

Polymorphism in pharmaceutical substances may affect both the efficacy and stability of a drug.<sup>2,3,7–16</sup> Specifically, the presence of different polymorphs with different dissolution rates in a solid dosage form may affect the uptake of the drug. In the case of liquid dosage forms the use of a metastable form of an active substance, with higher water solubility than the stable form, may lead to precipitation of the stable form and thus affect the shelf life of the drug product. Hence, the characterization of possible polymorphic forms and proper control of the presence of polymorphism in a drug substance are integral parts of the development of a new drug. Several reviews dealing with the occurrence of polymorphism in pharmaceutical substances have appeared.<sup>4,17,18</sup> A survey of the European Pharmacopoeia with respect to polymorphism<sup>19,20</sup> also gives a comprehensive list of references to the increasing number of case studies reported in recent years. A wide variety of approaches have been employed in such studies and a recent paper<sup>21</sup> gives guidance on how to prepare a comprehensive regulatory submission on the physicochemical properties of a pharmaceutical solid.

Organic polymorphs can be characterized by many different methods, such as microscopy, infrared spectroscopy, Raman spectroscopy, solid-state NMR spectroscopy, X-ray crystallography, thermal analysis and solubility and density measurements.<sup>5</sup>

In the present study the polymorphic forms of GdDTPA-BMA (gadodiamide) and DyDTPA-BMA (sprodiamide) are reported. Gadodiamide, a gadolinium chelate of diethylenetriamine pentaacetic acid bis(methylamide), is the active ingredient of OMNISCAN® (Nycomed Imaging AS, Oslo, Norway), a paramagnetic contrast medium for magnetic resonance imaging (MRI). Sprodiamide, the dysprosium analogue of GdDTPA-BMA, has also been evaluated as a potential contrast agent for MRI examinations.

## Experimental

**Samples.** Solid samples of gadodiamide and sprodiamide were taken from large-scale production batches prepared by precipitation from aqueous solution with acetone. Other samples were obtained by recrystallization from water or precipitation of aqueous solutions with ethanol or isopropyl alcohol. Amorphous samples were prepared by freeze-drying ( $7 \times 10^{-3}$  mmHg) of aqueous solutions.

The effect of the storage conditions (temperature, humidity) was investigated by keeping the substances under controlled conditions. Drying was performed at 60 °C in a vacuum chamber. The effect of humidity exposure was studied at three different conditions: 40 °C/75% relative humidity (RH), 25 °C/75% RH and 25 °C/60% RH for 10–14 days.

A total of 111 gadodiamide and 79 sprodiamide samples were investigated.

**Infrared spectroscopy.** Diffuse reflectance infrared spectra were recorded in the 4000–400  $\text{cm}^{-1}$  region on a Bruker IFS 66 FT-IR spectrometer equipped with a Harrick Scientific 'Praying Mantis' diffuse reflectance accessory. Samples were ground with potassium bromide (KBr) in an agate mortar (1–2% w/w), and the resulting powder was packed and levelled in the sample cup of the diffuse reflectance accessory. For each sample 256 scans were recorded at a resolution of 4  $\text{cm}^{-1}$ . The spectra were measured relative to a reference background obtained with pure KBr and transformed into the Kubelka–Munk format. The sample compartment of the infrared spectrometer was continuously flushed with dry air to avoid bands from atmospheric water. All samples of gadodiamide and sprodiamide were investigated by infrared spectroscopy.

**Raman spectrometry.** Raman spectra of solid gadodiamide were recorded with a Dilor Labram confocal microscope laser Raman spectrometer equipped with a 1800 line/mm grating. A few sample grains were placed under the microscope objective and illuminated by a He–Ne laser (632 nm). Spectra were recorded with 2 mW laser power and a slit width of 100  $\mu\text{m}$ .

Three gadodiamide samples were investigated by Raman spectroscopy.

**X-Ray diffractogram experiments.** The samples were pulverized in an agate mortar and spread out on Vaseline either on a silicon wafer or a Pt sample holder in the chamber of a high temperature sample device. The chamber could be evacuated in order to achieve a reduction of humidity. The samples were then investigated with monochromatic Cu  $K_{\alpha 1}$  radiation over the angular range  $2\Theta = 2\text{--}24^\circ$  in a Siemens D5000 diffractometer.

A total of 26 gadodiamide and 26 sprodiamide samples were investigated.

**Thermal analysis.** Differential scanning calorimetry (DSC) experiments were conducted with a Perkin Elmer DSC 7 calorimeter calibrated with In and Zn standards over the 20–350 °C temperature range. Approximately 3–5 mg of the sample were weighed in aluminium sample pans for volatile substances and immediately sealed and placed in the instrument. The samples were run in punctured pans under nitrogen purge and scanned in the temperature range from 20 to 250 °C with a heating rate of 10 °C  $\text{min}^{-1}$ .

Thermogravimetric analysis (TGA) was carried out under nitrogen purge in the temperature range 27–600 °C with a heating rate of 20 °C  $\text{min}^{-1}$  on a Perkin Elmer TGA 7 thermogravimetric analyser.

A total of 15 gadodiamide and 6 sprodiamide samples were investigated by DSC and TGA.

**Water content.** The water content (% w/w) was determined by the Karl–Fischer titration method. The water uptake of gadodiamide I was investigated gravimetrically by storage of a sample with an initial water content of 11.4% w/w at 25 °C and different relative humidities (0, 22, 40, 75 and 93%).

**Solubility determination.** Saturated aqueous solutions of gadodiamide and sprodiamide samples were prepared by stirring excess solid in water at room temperature. The concentration (in  $\text{mg mL}^{-1}$ ) of the samples was determined by liquid chromatography [column, Supelcosil LC-18-DB (5  $\mu\text{m}$  particles, 25–30 cm length); mobile phase, 5 mM triethylammonium acetate; post-column reagent, 0.06 mg Arsenazo III per mL; flow rate, 1.5  $\text{mL min}^{-1}$ ; detection, at 658 nm; sensitivity, 0.1 AUFS] after 0.5, 4 and 20 h. For amorphous gadodiamide and sprodiamide, the solubility was determined after 15 and 5 min, respectively.

## Results

Gadodiamide (Fig. 1) is normally obtained as a white solid consisting of small, needle-like crystals. In large-scale manufacturing such crystals are obtained by addition of acetone to an aqueous solution of gadodiamide, but precipitation giving needle-like crystals may also be

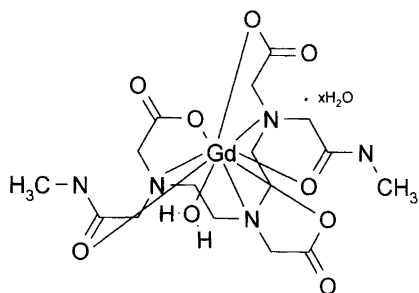


Fig. 1. Structure of GdDTPA-BMA (gadodiamide).

induced by other solvents (ethanol, isopropyl alcohol). However, when gadodiamide was precipitated in the laboratory without the addition of an organic solvent, rock-like, almost colourless crystals were occasionally obtained. Drying of these crystals gave a white material which did not consist of needles when examined under a microscope. Depending on the crystallization procedure, therefore, different habits of solid gadodiamide were obtained. The goal of this investigation was to examine if these habits also represented different modifications (polymorphs) of gadodiamide.

*GdDTPA-BMA.* The infrared and Raman spectra of solid gadodiamide are shown in Figs. 2–4. Tabulated wavenumber positions and a tentative interpretation of the main absorptions are given in Table 1. In addition to the three types of spectra corresponding to solid phases which were stable under ambient conditions [denoted type I (the normal form), II (obtained after drying of III) and III (the rocklike, colourless crystals)], two spectra (types IV and V) appeared on drying of the powdered II and I samples dispersed in KBr in the dry

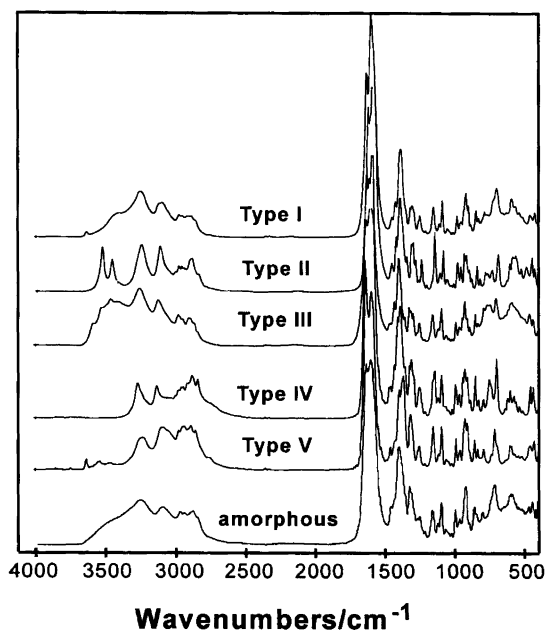


Fig. 2. Infrared spectra (Kubelka Munk units) of the gadodiamide polymorphs.

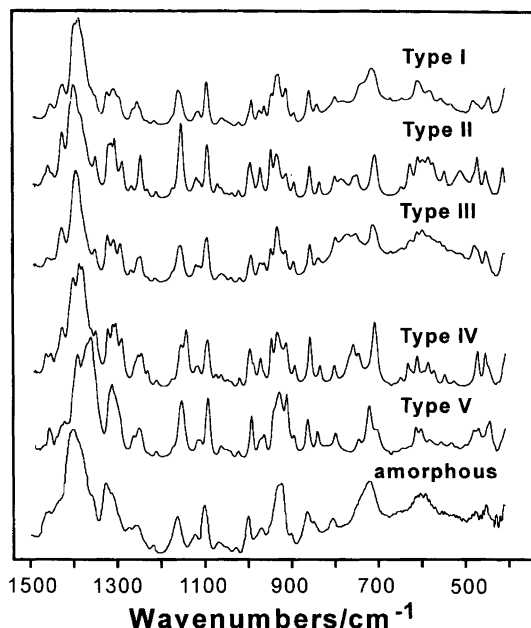


Fig. 3. Expanded infrared spectra (Kubelka Munk units) of the gadodiamide polymorphs.

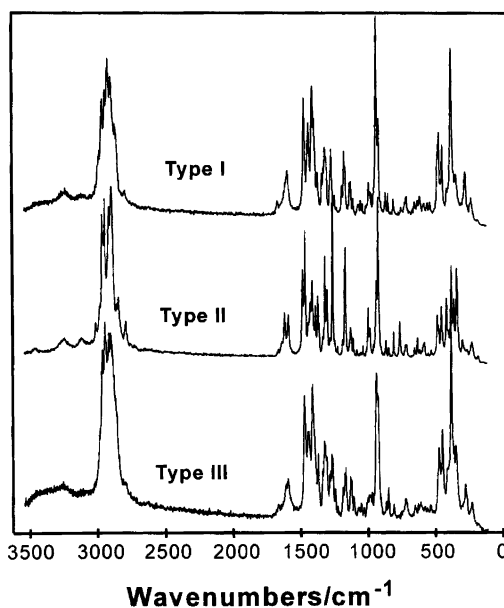


Fig. 4. Raman spectra of gadodiamide polymorphs.

air atmosphere of the infrared spectrometer. The infrared and Raman spectra show differences particularly in the OH stretching bands ( $3700\text{--}3300\text{ cm}^{-1}$ ), but also in the fingerprint region ( $1500\text{--}450\text{ cm}^{-1}$ ). When exposed to the conditions in the IR spectrometer, complete conversion from II to IV and I to V took place in about 40 min, and both were reversibly transformed into the original forms when re-exposed for 10 min to the ambient humidity in the laboratory. In comparison, the recording of the infrared spectra took about 3 min. When subjected to the dry air atmosphere of the infrared spectrometer the type III spectrum first changed into a type II spec-

Table 1. Infrared and Raman spectral data for gadodiamide polymorphs (s, strong; m, medium; w, weak; v, very; b, broad; sh, shoulder).

Tentative assignment	Type I		Type II		Type III	
	IR	Raman	IR	Raman	IR	Raman
Coordinated water	3642 w	3640 vwb			3580 w	
Coordinated water			3531 s	3528 w	3531 w	
Coordinated water			3463 s	3462 mw	3463 w	3450 wb
Lattice water	3410 mb	3400 wb			3400 mb	
Amide ( <i>trans</i> ) N-H	3263 sb	3250 wb	3251 sb	3245 wb	3258 sb	3250 wb
Amide II overtone	3129 sb		3121 s	3121 w	3124 sb	
	2984 m	2985 m	2988 s	2985 s	2978 m	2985 sh
CH <sub>3</sub> antisym. str.	2960 sh	2965 s	2968 sh	2966 vs	2960 sh	2967 s
		2945 s	2951 w	2950 s	2948 w	2946 vs
CH <sub>2</sub> antisym. str.	2915 m	2925 vs	2900 sh	2914 s	2908 m	2919 s
CH <sub>3</sub> sym. str.	2895 m	2900 s	2894 m	2894 vs	2890 sh	2905 s
CH <sub>2</sub> sym. str.	2865 sh	2870 m	2848 sh	2850 sh	2868 w	2865 sh
Amide I	1642 vs	1670 vw	1640 vs	1640 sh	1641 vs	1660 w
Carboxylate antisym. C-O	1610 vs	1610 m	1600 vs	1612 m	1608 vs	1595 m
Amide II	1590 sh	1590 m		1584 m		
CH <sub>3</sub> /CH <sub>2</sub> def.	1465 w	1470 s	1469 w	1469 ms	1460 w	1467 s
	1433 m	1440 ms	1439 m	1459 s	1441 m	1435 ms
Carboxylate sym. C-O	1410 s	1415 s	1408 s	1408 s	1406 s	1404 s
	1397 s	1400 sh				
		1370 w		1366 m		1366 w
	1333 m	1315 m	1329 m	1313 s	1332 m	1318 m
	1262 m	1265 m	1253 m	1253 vs	1262 m	1261 m
Antisym. CNC str.	1167 m		1158 s	1158 s	1166 m	1158 m
				1120 m		1125 m
	1098 m		1096 ms	1100 w	1097 m	
	994 m		996 m		994 m	
Sym. CNC str.	930 m	928 vs	948 ms	927 s	933 ms	927 s
		915 s		915 s		914 sh
	859 m	865 w	858 m	857 w	857 m	856 w
		845 w		835 m		840 w
		800 w		800 w		800 w
		740 w		753 w		
	713 m	705 w	705 ms	703 w	711 m	710 w
				621 w		
		464 m		464 ms		462 m
		433 m		442 ms		434 m
		372 s		368 s		368 vs
				349 s		350 sh
		330 w		325 ms		335 m
		260 w		285 w		266 w
		215 w		212 w		215 w
				164 w		

trum, which in turn could be reversibly transformed to a type IV spectrum as observed with the pure type II sample. The infrared spectrum of the freeze-dried sample had considerably broader bands than the other solids, as expected for an amorphous sample (Figs. 2 and 3).

Five different powder diffractograms were obtained when gadodiamide types I-V were analysed by X-ray (Fig. 5). The type I-III diffractograms again refer to the three forms which could be isolated in the laboratory. The reversible conversion of types I and II to types V and IV, respectively, were reflected by appropriate changes in the diffractograms when X-ray experiments were performed with samples kept in a sample chamber with variable humidity. Thus, the changes observed in the infrared spectra were confirmed by changes in the

X-ray diffractograms. The amorphous nature of solid gadodiamide obtained by freeze-drying was confirmed by an X-ray diffractogram completely devoid of peaks.

The DSC analysis of gadodiamide I (five samples) showed two endotherms with peak temperatures of  $T_m = 115-135^\circ\text{C}$  ( $\Delta H = 135-170 \text{ J g}^{-1}$ ) and  $T_m \approx 240^\circ\text{C}$ . The two DSC transitions were accompanied by weight losses in the TGA curves of 9 and 2.5% w/w, respectively. For gadodiamide II only one DSC endotherm ( $T_m = 104-107^\circ\text{C}$ ,  $\Delta H = 46-58 \text{ J g}^{-1}$ ) and one TGA weight loss (ca. 5-6% w/w) was observed. As opposed to samples of types I and II, gadodiamide III showed two DSC peaks in the  $50-150^\circ\text{C}$  temperature range (80-110 and  $110-135^\circ\text{C}$ ,  $\Delta H = 106-461 \text{ J g}^{-1}$ ). The corresponding TGA curve of a type III solid showed an approximately

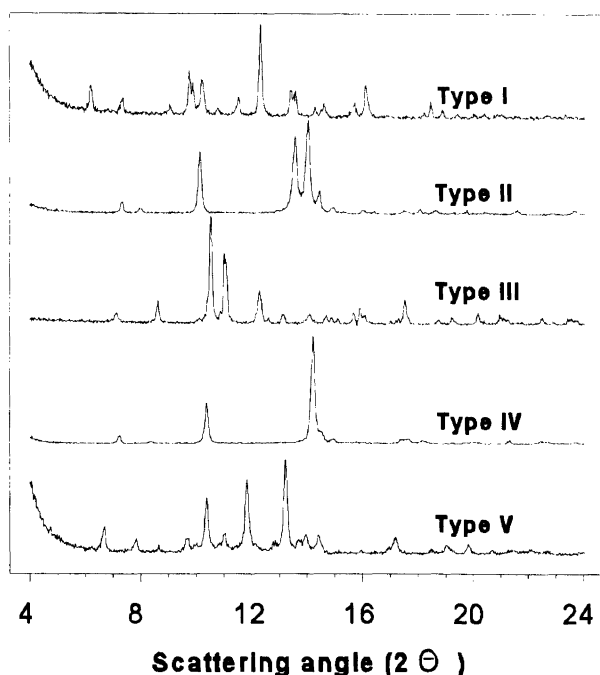


Fig. 5. Powder X-ray diffractograms of the gadodiamide polymorphs.

10% w/w weight loss occurring around 100–150 °C. The position and relative intensity of the two DSC peaks varied somewhat between the samples investigated. A DSC endotherm at ca. 260 °C and a corresponding 2% TGA weight loss was observed in one of the type III samples, but these processes were absent in the other two samples investigated. Sample decomposition started at ca. 300–320 °C as revealed by a dramatic weight loss in the TGA curves of type I–III samples. Amorphous gadodiamide showed a broad endotherm (from 65 to 155 °C).

Table 2 summarizes the TGA results and the water content observed in gadodiamide types I–III and amorphous gadodiamide. The water content was determined in almost all samples, whereas a relatively small selection of samples was studied by TGA. This explains the narrow ranges observed by TGA. For gadodiamide type II the water content is concentrated around zero, one and two water molecules per gadodiamide molecule. Gadodiamide type III had a water content corresponding to seven water molecules per gadodiamide unit, whereas gadodiamide I formed hydrates corresponding to one,

Table 2. Water content and TGA weight loss of gadodiamide (GdDTPA-BMA · x H<sub>2</sub>O) polymorphs.

Polymorph	Water content (Karl Fischer)		TGA weight loss
	Molar ratio (x)	%(w/w)	%(w/w)
Type I	1–5	3–14	12
Type II	0–2	1–6	5–6
Type III	7	18	11–14
Amorphous	1–7	3–18	10

two, four and five molecules of water per chelate unit. However, four and five water molecules were predominant for gadodiamide I. Figure 6 shows the results from the water uptake study of gadodiamide type I. The initial water content (11.4% w/w) dropped significantly in the samples stored at 0% RH. At high humidities, the water content levelled out at ca. 13% w/w, which corresponds to a pentahydrate.

The water solubilities of gadodiamide types I–III and amorphous material are compiled in Table 3. For gadodiamide II and gadodiamide III the maximum solubility was observed after 4 h of stirring of a saturated solution. Amorphous gadodiamide had a high dissolution rate and showed a maximum solubility after only 15 min of stirring, followed by a massive precipitation after an additional 15 min. Infrared spectroscopy showed this precipitate to be gadodiamide III. The results show that type I gadodiamide is the least soluble, with gadodiamide II slightly more soluble than gadodiamide III.

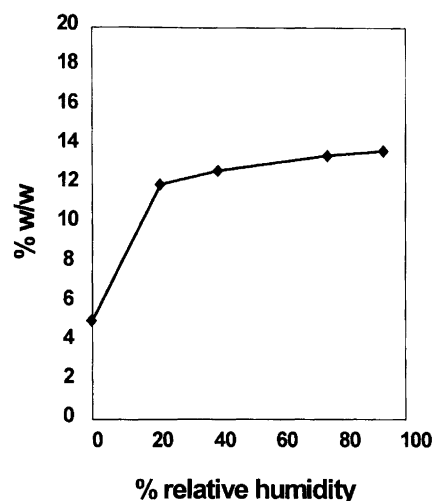


Fig. 6. The water content of gadodiamide I as a function of relative humidity.

Table 3. The different solubilities of gadodiamide (GdDTPA-BMA · x H<sub>2</sub>O) and sprodiamide (DyDTPA-BMA · x H<sub>2</sub>O) polymorphs in water.

Polymorph	Time/h	Solubility/mg mL <sup>-1</sup>	
		GdDTPA-BMA · x H <sub>2</sub> O	DyDTPA-BMA · x H <sub>2</sub> O
Type I	0.5		
	4		490
	20	469	
Type II	0.5	544	
	4	571	481
	20	564	
Type III	0.5	522	
	4	554	483
	20	530	
Amorphous	0.1		979
	0.25	784	

Amorphous gadodiamide had a significantly higher solubility in water than the crystalline forms.

The formation of gadodiamide **II** by drying of gadodiamide **III** at 60 °C was demonstrated to be both rapid and complete. Usually no transformations among types **I**, **II** and **III** were seen under normal laboratory conditions. In one case a long-term conversion of gadodiamide **III** to gadodiamide **I** was observed. Infrared spectra showed that a sample containing gadodiamide **III** with traces of gadodiamide **I** was transformed into pure gadodiamide **I** after 8 months of storage in a closed container at room temperature. No data were available during the 8 months of storage, and it is therefore not known if the transformation of this particular sample went directly from **III** to **I** or via a type **II** intermediate. However, infrared spectroscopy showed that mixtures of types **II** and **III** gadodiamide could be obtained by storage of gadodiamide **III**. Hence it is possible that the transformation from gadodiamide **III** to gadodiamide **I** goes via gadodiamide **II**.

At 40 °C/75% RH gadodiamide **III** and gadodiamide **II**, as well as the amorphous substance, were irreversibly transformed into gadodiamide **I**. At 25 °C/60% RH the situation was different: Gadodiamide **III** remained unchanged, gadodiamide **II** was converted into gadodiamide **III** and amorphous gadodiamide absorbed water. On the other hand, upon storage at 25 °C/75% RH gadodiamide **II** was converted to gadodiamide **I**. Figure 7 summarizes the observed conversion pathways between the different gadodiamide polymorphs.

*DyDTPA-BMA*. In general, the experimental results for sprodiamide were very similar to those of gadodiamide. This is illustrated by the infrared spectra of gadodiamide **I** and sprodiamide **I**, which are essentially identical

(Fig. 8). The infrared spectra and the X-ray diffractograms of the crystalline forms of sprodiamide and of amorphous sprodiamide exhibited identical patterns to those of the corresponding gadodiamide forms. Among the sprodiamide samples studied, some had infrared spectra which could be interpreted as a superposition of a type **II** and a type **III** spectrum. The water contents of these samples were also between typical type **II** and type **III** values. X-Ray diffraction results confirmed that these specimens were mixtures of the type **II** and **III** solids and not a sixth polymorph.

The experiments showed that type **III** sprodiamide was much more frequently encountered than gadodiamide **III**. Precipitation of an aqueous sprodiamide solution with acetone gave either type **I** or **III** solids, as opposed

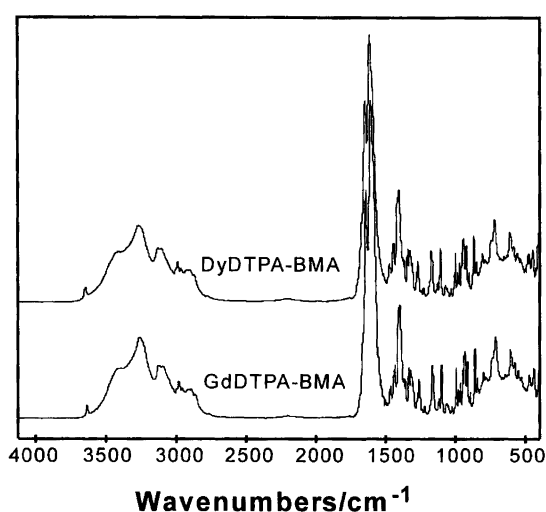


Fig. 8. Infrared spectra (Kubelka Munk units) of gadodiamide **I** and sprodiamide **I**.

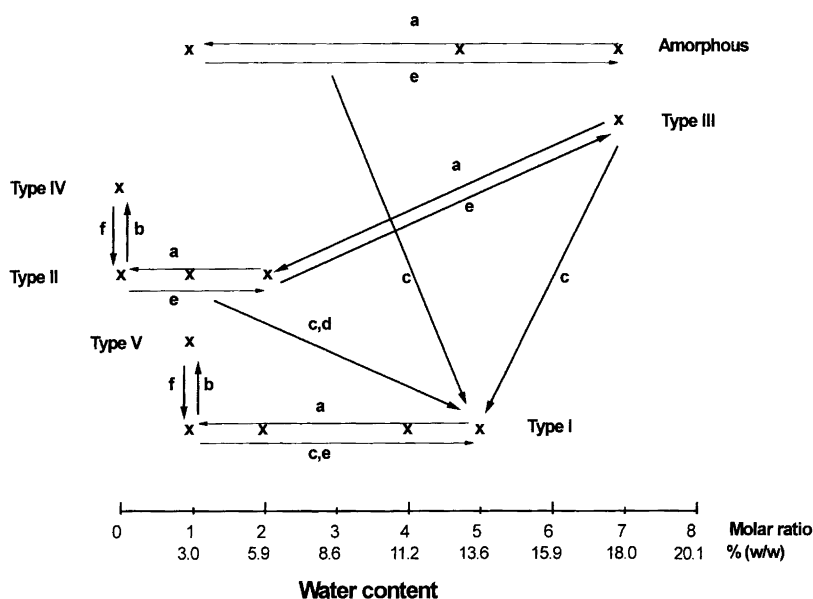


Fig. 7. Observed water contents ( $x$ ) and conversion pathways between gadodiamide polymorphs. (a) 60 °C/vacuum; (b) dry air or vacuum; (c) 40 °C/75%RH; (d) 25 °C/75%RH; (e) 25 °C/60%RH; (f) exposure to ambient atmosphere.

to gadodiamide, which invariably precipitated as type I. Precipitation of sprodiamide from water without the addition of an organic solvent gave only the type III form, whereas gadodiamide gave both gadodiamide I and III under these conditions.

The DSC/TGA curves of sprodiamide I, II and III were also analogous to the corresponding gadodiamide results. Sprodiamide I showed two DSC endotherms with peak temperatures of  $T_m = 111^\circ\text{C}$  ( $\Delta H = 131\text{ J g}^{-1}$ ) and  $T_m \approx 220^\circ\text{C}$ , sprodiamide II had a single DSC transition at  $T_m = 105\text{--}113^\circ\text{C}$  ( $\Delta H = 49\text{--}87\text{ J g}^{-1}$ ), whereas two overlapping transitions were observed in sprodiamide III ( $T_m = 97\text{--}129^\circ\text{C}$ ,  $\Delta H = 350\text{--}450\text{ J g}^{-1}$ ). The results given in Table 2 also apply to sprodiamide, with the exception that the observed 17–18% weight loss in TGA runs of sprodiamide III showed better agreement with the Karl–Fischer water content than the gadodiamide III results.

In the sprodiamide case the solubilities of types I–III are almost identical (Table 3), while amorphous sprodiamide is much more soluble. Amorphous sprodiamide also had a very high dissolution rate. The solubility of amorphous sprodiamide was determined after 5 min. After 15 min a massive precipitation of sprodiamide III occurred, analogous to what happened with gadodiamide.

Transitions between polymorphs were also investigated, and Fig. 7 also applies to sprodiamide, but with one exception: storage of sprodiamide type II at  $25^\circ\text{C}/75\%$  RH resulted in conversion to type III, not the type I polymorph as observed with gadodiamide.

Samples of sprodiamide I–III were stored well separated in the same beaker at  $25^\circ\text{C}/40\%$  RH (conditions close to normal laboratory conditions) for 16 weeks. No transformations between forms were seen under these conditions. The water contents in type I and type III were stable (12% and 18%, respectively), while the water content in type II increased from 1 to 7%.

## Discussion

Once the purity of the samples is established, powder X-ray diffraction is the method of choice for differentiation between crystalline modifications of a solid.<sup>17</sup> The X-ray diffractograms (Fig. 5) confirmed the crystallinity of the type I–V solids and the amorphous nature of the freeze-dried solids. Characteristic X-ray diffraction patterns with respect to the number of peaks and their  $2\theta$  values were obtained for the five different types (Fig. 5). From this it can be concluded that they represented five different polymorphic forms. The wide range of water contents observed with the type I polymorphs (Table 2 and Fig. 7) did not influence the appearance of the X-ray diffractograms. The effect of water content on the infrared spectrum of the type I solids could be seen as an enhancement of the broad O–H band at approximately  $3400\text{ cm}^{-1}$  superimposed on the typical gadodiamide/sprodiamide type I spectrum. Hence, these solids

were interpreted as pseudopolymorphs of the type I polymorph.

The DSC and TGA results for gadodiamide I and sprodiamide I (Table 2) showed a weight loss in the  $100\text{--}150^\circ\text{C}$  range which was attributed to a loss of lattice water (9% by weight, corresponding to three water molecules per chelate molecule). The observed transition is probably also accompanied by a phase transition from a type I to a type V solid in accordance with observations in the dry air atmosphere of the infrared spectrometer. The second DSC endotherm ( $220\text{--}240^\circ\text{C}$ ) and the corresponding 2.5% TGA weight loss were interpreted as a loss of coordinated water (the water molecule directly connected to the metal), which may be due to an anhydrous pseudopolymorph of type V, or the formation of a new polymorph VI. This can not be decided without supporting data from powder X-ray and IR. Remaining OH stretching bands were seen in the  $3530\text{--}3640\text{ cm}^{-1}$  range of the type V spectrum, suggesting that the relatively gentle drying of the substance in the infrared spectrometer does not remove all the water present in the type V solid. The situation with the type V solid is remarkably similar to that of a HMG-CoA reductase inhibitor which also showed a band at  $3640\text{ cm}^{-1}$  attributed to bound water that could only be made to disappear upon heating.<sup>22</sup>

The type II solids showed only one DSC endotherm ( $104\text{--}107^\circ\text{C}$ ) and a corresponding TGA weight loss of 5–6%. This was interpreted as a loss of two water molecules present in gadodiamide II and sprodiamide II and a concurrent transformation into the type IV polymorph. The O–H stretching region of the infrared spectra (Fig. 2) revealed a complete lack of water in the type IV polymorph which was obtained by relatively gentle drying of the type II solid. This explains why no further TGA weight loss or DSC endotherms were observed in the type II polymorphs at higher temperatures. Diffraction quality crystals of the type II polymorphs have not yet been obtained, so the distribution of lattice water and coordinated water in these crystals is unknown. However, some conclusions may be drawn from the infrared spectra. The type II spectrum (Fig. 2) showed two sharp peaks at  $3531\text{ cm}^{-1}$  and  $3462\text{ cm}^{-1}$  whose sharpness suggests that they are due to water molecules distributed in the crystal in an ordered manner. The band positions show that the water molecules are hydrogen bonded. The absence of a broad O–H stretching contour, like the one seen in the spectra of the amorphous solid as well as the type I and type III polymorphs, shows that there is no appreciable amount of randomly oriented water molecules in the type II polymorphs.

In accordance with the DSC and TGA results obtained on the type I and II polymorphs of both gadodiamide and sprodiamide, one would expect to see two transitions in the  $100\text{--}150^\circ\text{C}$  range of the type III solids, one representing a water loss and transformation from type III to type II and a second peak representing the final loss of water and a transformation into the type IV

polymorph. This was indeed observed in all of the type **III** solids investigated. The TGA weight loss observed with the sprodiamide type **III** solids correlated well with the water content determined by the Karl–Fischer method, whereas the gadodiamide type **III** solids generally gave a lower TGA weight loss than expected from the Karl Fischer results.

Water may be present in a crystal either as lattice (interstitial) water or coordinated water,<sup>23</sup> although there is no definitive borderline between the two. The former denotes water molecules trapped in the crystal lattice either by hydrogen bonds or weak ionic bonds, whereas the latter refers to water molecules coordinated by partially covalent bonds to a metal. The lattice water molecules will form hydrogen bonds both to the ligand oxygens and to other water molecules. The presence of both interstitial and coordinated water has been confirmed by X-ray crystallography both on gadodiamide<sup>24</sup> and sprodiamide.<sup>25</sup> The polymorphic identity of the material was not known at the time when the cited crystallographic studies were carried out, and repeated studies with known polymorphic material are in progress.<sup>26</sup> The published crystallographic data<sup>24,25</sup> showed, however, that one water molecule is coordinated directly to the lanthanide. Indeed, the efficacy of gadodiamide as a magnetic resonance contrast agent relies on the fact that water molecules may interact directly with the ninth coordination site on gadolinium.<sup>24</sup> Lanthanide chelate complexes generally show coordination numbers ranging from 8 to 10.<sup>27</sup> From the water content, IR spectra and the DSC/TGA results it is evident that the coordinated water is more loosely bound in type **II** than in type **I**. Type **II** has been seen with water contents of 0.5%, and the last remains of water is lost below 150 °C, upon formation of completely anhydrous type **IV**. In contrast, type **I** has not been observed with water contents below 3%, and type **V** still contains traces of water as revealed by the infrared spectra (see also Fig. 7). The coordinated water in the type **I**–type **V** system is lost in the 200–250 °C interval.

The values for the water solubility are somewhat uncertain and must be considered as minimum values due to the fact that a saturated solution of a given polymorph will represent a supersaturated system with respect to a less soluble polymorph.<sup>15,21</sup> In fact, the solutions of types **II** and **III** gadodiamide were seen to pass through a maximum concentration value followed by a gradual decrease due to conversion to type **I**, which is less soluble (Table 3). The fast dissolution rates and the high solubilities of amorphous gadodiamide and sprodiamide are in accordance with the low stability of these forms.

The dynamic nature of the transformations between the different polymorphic forms is revealed by the drying and humidity experiments. Almost all transformations were reversible given the right conditions, except the **II**→**I**, **III**→**I** and amorphous material→**I** transformations which were found to be irreversible. This shows that type **I** is the thermodynamically most stable form;

once it is formed it can not be converted back to type **II**, type **III** or amorphous material. Type **I** only converts reversibly to the unstable type **V** solid. The water solubilities confirm this conclusion in that the type **I** solid also had the lowest solubility. This can be rationalized by arguing that the stable form has the greatest resistance towards change, such as solubilization or melting.

The more frequent occurrence of sprodiamide **III** and **II** as compared to gadodiamide **III** and **II** indicates that types **I**–**III** are closer in energy in the case of sprodiamide. This is supported by two facts: the water solubilities of sprodiamides **I**–**III** are almost identical (Table 3), and sprodiamide **II** is more prone to convert into the type **III** form when exposed to humidity than gadodiamide **II**.

Whether type **II** polymorph will convert to type **III** or type **I** may depend both on relative stabilities as well as the energy barriers between the polymorphs. The transformation of polymorph **II** to **III** and **I** seems to be governed by kinetic and thermodynamic control, respectively. Under mild conditions the thermodynamically metastable polymorph **III** is formed by kinetic control, whereas the thermodynamically more stable polymorph **I** is formed under more compelling conditions. This indicates that the **II**→**III** transformation has a lower activation barrier than the **II**→**I** transformation. When two polymorphic forms can be reversibly transformed into each other, they are said to be in an enantiotropic relationship, whereas when the transformation between two forms is irreversible, the forms are said to be in a monotropic relationship.<sup>4,6,9,12,13,16,28</sup> In the gadodiamide and sprodiamide systems all transformations are enantiotropic, except the **II**→**I**, **III**→**I** and amorphous material→**I** transformations which are monotropic. By proper treatment all metastable forms can be transformed to the stable form **I**.

*Acknowledgements.* Thanks are due to Yemane Haile and Vera Kasparikova (Nycomed Imaging AS), Trine-Lise Rolfsen (SINTEF) and Hans-Jürgen Reich (DILOR GmbH) for skilful technical assistance. Nycomed Imaging AS is acknowledged for the permission to publish the present study.

## References

1. McCrone, W. C. In Fox, D., Labes, M. M. and Weissberger, A., Eds., *Physics and Chemistry of the Organic Solid State*, Interscience, New York 1965; Vol. II, pp. 725–768.
2. Giron, D. *Mol. Cryst. Liq. Cryst.* 161 (1988) 77.
3. Jain, N. K. and Mohammedi, M. N. *Indian Drugs* 23 (1986) 315.
4. Haleblan, J. and McCrone, W. J. *J. Pharm. Sci.* 58 (1969) 911.
5. Threlfall, T. L. *Analyst (London)* 120 (1995) 2435.
6. Dunitz, J. D. and Bernstein, J. *Acc. Chem. Res.* 28 (1995) 193.
7. Burger, A. *Top. Pharm. Sci.* 43 (1983) 347.
8. Pearson, J. T. and Varney, G. *Manuf. Chem. Aerosol News* 44 (1973) 36.



9. Rao, B. R., Rao, G. R. and Avadhanulu, A. B. *J. Sci. Ind. Res.* 46 (1987) 450.
10. Burger, A. *Oesterr. Apoth. Ztg.* 31 (1977) 1050.
11. Thoma, K. and Serno, P. *Dtsch. Apoth. Ztg.* 124 (1984) 2162.
12. Mewada, G. S., Parikh, D. R. and Somasekhara, S. *Sci. Cult.* 39 (1973) 378.
13. Muzaffar, N. A. and Afzal Sheikh, M. *J. Pharm. (Lahore)* 1 (1979) 59.
14. Chorpa, K. S. and Dhall, V. K. *Pharmacos* 25 (1981) 39.
15. Clements, J. A. *Proc. Anal. Div. Chem. Soc.* 13 (1976) 21.
16. Rosenstein, S. and Lamy, P. P. *Am. J. Hosp. Pharm.* 26 (1969) 598.
17. Haleblan, J. K. *J. Pharm. Sci.* 64 (1975) 1269.
18. Borcka, L. and Haleblan, J. K. *Acta Pharm. Jugosl.* 40 (1990) 71.
19. Borcka, L. *Pharm. Acta Helv.* 66 (1991) 16.
20. Borcka, L. *Pharmeuropa* 7 (1995) 574, 586.
21. Byrn, S., Pfeiffer, R., Ganey, M., Hoiberg, C. and Poochikian, G. *Pharm. Res.* 12 (1995) 945.
22. Morris, K. R., Newman, A. W., Bugay, D. E., Ranadive, S. A., Singh, A. K., Szyper, M., Varia, S. A., Brittain, H. G. and Serajuddin, A. T. M. *Int. J. Pharm.* 108 (1994) 195.
23. Nakamoto, K. *Infrared and Raman Spectra of Inorganic and Coordination Compounds*, 4th edn., Wiley, New York 1986, pp. 227–231.
24. Chang, C. A. *Invest. Radiol.* 28S (1993) S21.
25. Ehnebom, L. and Pedersen, B. F. *Acta Chem. Scand.* 46 (1992) 126.
26. Aukrust, A., Sydnes, L. K. and Sæthre, L. J. *To be published.*
27. Rocklage, S. M. and Watson, A. D. *J. Magn. Reson. Imaging* 3 (1993) 167.
28. Burger, A. *Pharm. Int.* 3 (1982) 158.

Received December 11, 1996.